Supplementary Figures 1-4

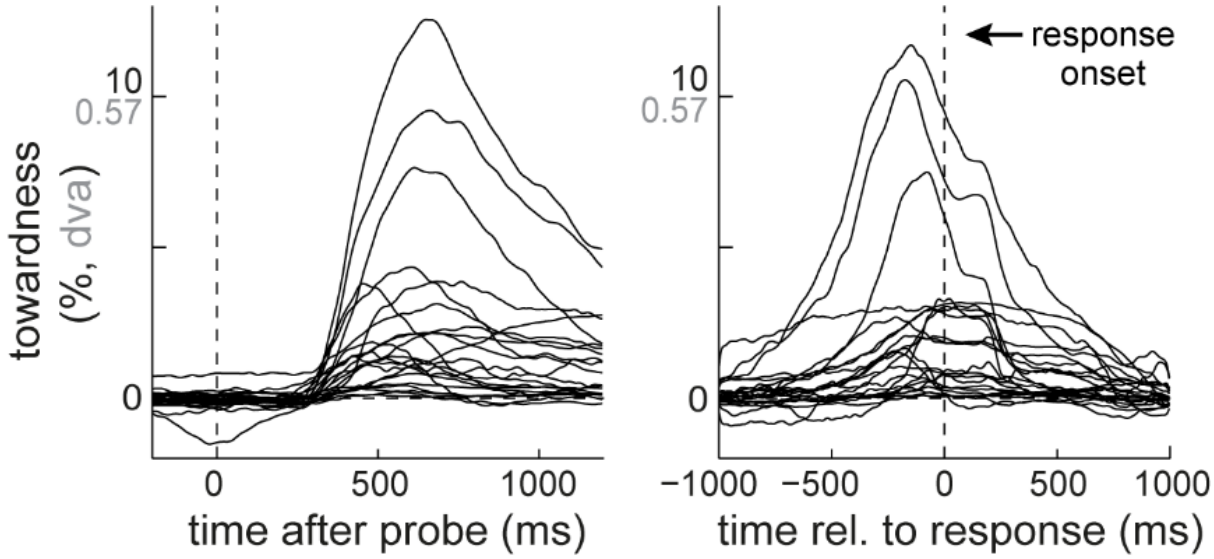

Supplementary Figure 1 | Individual participant gaze time courses in experiment 1. Single-participant data underlying the average gaze bias depicted in **Fig. 1c** and **Fig. 1d**. Each trace reflects one participant (n = 23). Percentages are defined relative to the items' centre locations at encoding, with 100% corresponding to approximately 5.7 degrees visual angle (denoted "dva"). To enhance interpretability, we depict both metrics on all axes that involve gaze position or gaze shift magnitude information (percentage in black; degrees of visual angle in grey).

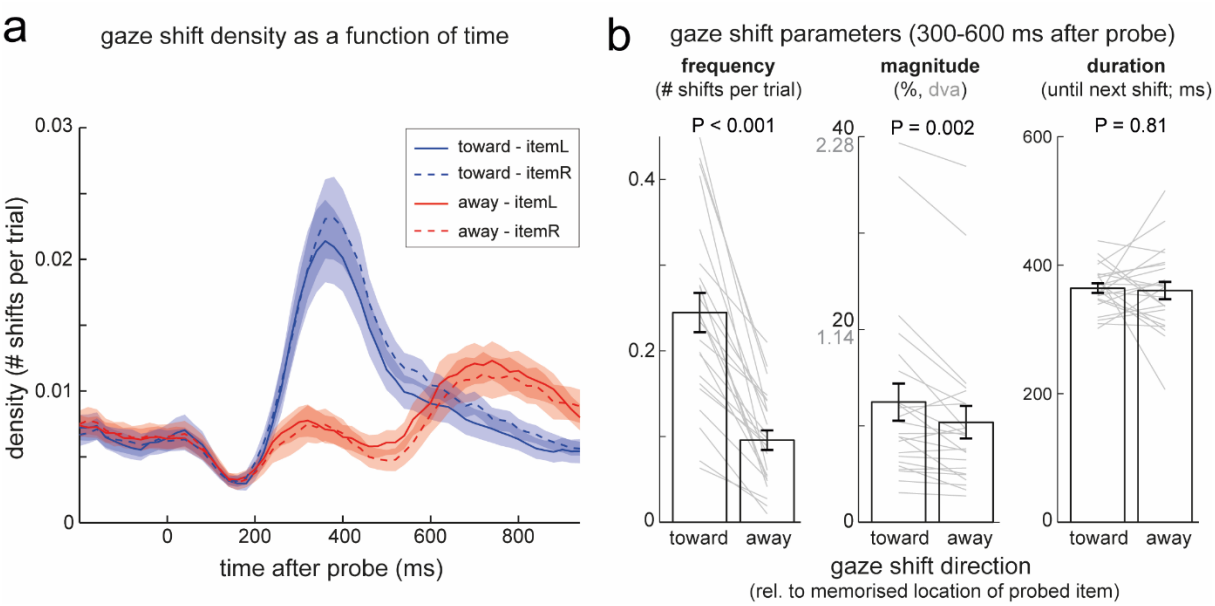

Supplementary Figure 2 | Time course of gaze shifts, and average gaze shift frequency, magnitude, and ensuing fixation durations for identified shifts toward and away from the memorised location of the probed item. a) Time course of gaze shift density for shifts toward (same direction) and away from (opposite direction) the memorised location of the probed memory item. We used a 100-ms sliding time window that was advanced in steps of 20 ms. Note that the relative dominance of 'away' shifts after 600 ms likely reflects the return of gaze to the centre. **b)** The identified gaze-position bias appears most strongly driven by an increased frequency of gaze shifts in the direction of the memorised location of the probed item ($t_{(19)}$ = 8.058, P < 0.001, d = 1.68, 95%CI of d between 1.032 and 2.313) supplemented by a smaller, but still significant, increase in average gaze-shift magnitude ($t_{(19)}$ = 3.576, P = 0.002, d = 0.746, 95%CI of d between 0.275 and 1.203). We did not observe any direction-depended difference in ensuing fixation durations – quantified as time after each identified gaze-shift until the detection of the next gaze shift ($t_{(19)}$ = 0.25, P = 0.805, d = 0.052, 95%CI of d between -0.357 and 0.461). We concede that the exact values here will inevitably depend on the exact time window for which gaze shifts are included, as well as on our ability to detect and classify individual gaze shifts accurately. Grey lines show individual participant data. Shading and error bars represent ± 1 s.e.m (n = 20). Data from experiment 1.

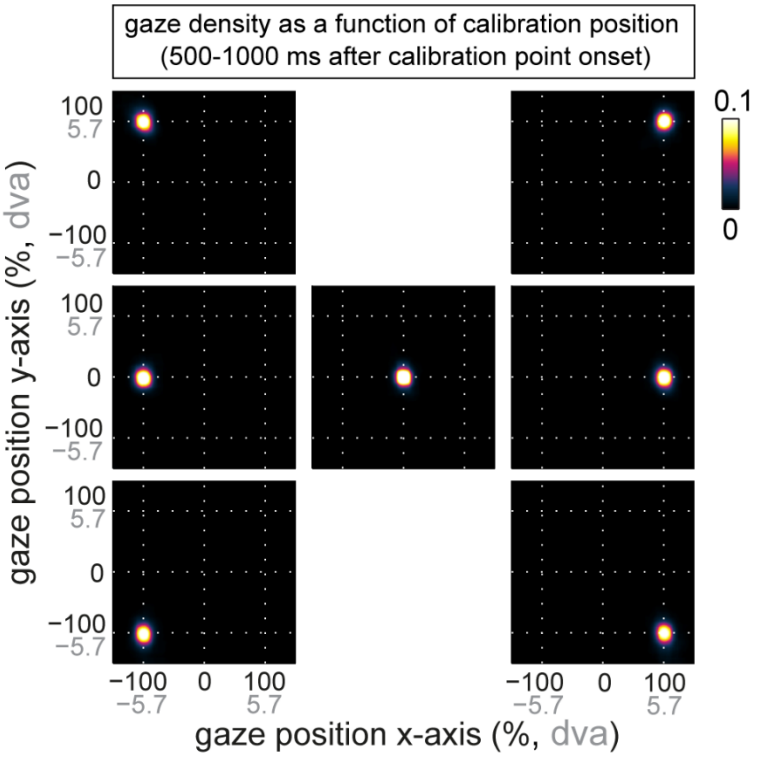

Supplementary Figure 3 | Gaze-calibration data. Average gaze position density during gaze calibration modules as a function of calibration position. Positions were chosen to match the centre of the bar stimuli used in each experiment and were accordingly defined as ±100 percent. The same calibration procedure and positions were used in all four experiments. Data from experiment 1.

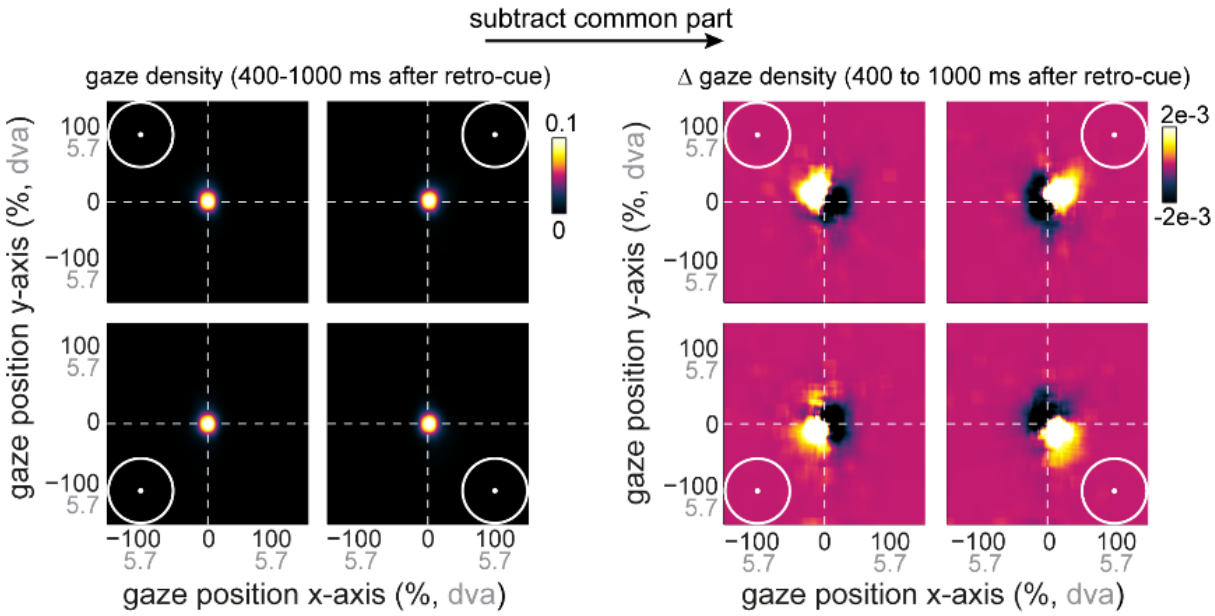

Supplementary Figure 4 | Gaze heat maps before and after subtraction of the common part, following informative retro-cues in experiment 2. Density of two-dimensional gaze position following probes of left-top, right-top, left-bottom, and right-bottom items, before and after subtraction of the density values that were shared between all four memorised locations. White circles indicate the area occupied by the probed item at encoding. Percentages are defined relative to the items' centre locations at encoding, with 100% corresponding to approximately 5.7 degrees visual angle (denoted "dva"). To enhance interpretability, we depict both metrics on all axes that involve gaze position or gaze shift magnitude information (percentage in black; degrees of visual angle in grey).